10442 *Macromolecules* **2010**, *43*, 10442–10451
DOI: 10.1021/ma100921s

Macromolecules
ARTICLE

Amphiphilic Poly(ethylene oxide)-*block*-poly(butadiene-*graft*-liquid crystal) Copolymers: Synthesis and Self-Assembly in Water

Hong Yang,[†,‡] Lin Jia,[†] ChenHui Zhu,[§] Aurelie Di-Cicco,[†,⊥] Daniel Levy,[†,⊥] Pierre-Antoine Albouy,[∥] Min-Hui Li,[†] and Patrick Keller*[,†,○]

[†]*Institut Curie, Centre de Recherche, CNRS UMR 168, Université Pierre et Marie Curie 26 rue d'Ulm 75248 Paris Cedex 05, France,* [‡]*School of Chemistry and Chemical Engineering, Southeast University, Nanjing 211189, China,* [§]*Department of Physics, University of Colorado, 390 UCB, Boulder Colorado 80309-0390, United States ,* [⊥]*Cell and tissue imaging (Pict-IBiSA), Institut Curie, Paris, France,* [∥]*Université Paris-Sud, CNRS UMR 8502, Laboratoire de Physique des Solides, 91405 Orsay cedex, France, and* [○]*Department of Chemistry and Biochemistry, University of Colorado, Boulder Colorado 80309-0215, United States*

Received April 27, 2010; Revised Manuscript Received November 18, 2010

ABSTRACT: What could be the self-assembly behavior in aqueous solution for an amphiphilic block copolymer with a very flexible hydrophobic backbone possessing however a liquid crystalline (LC) order? To answer this question, five amphiphilic block copolymers were prepared by grafting, via a thiol−ene addition reaction, four different thiol-functionalized LC mesogens or LC-like side groups on two commercially available poly(ethylene oxide)-*block*-poly(butadiene) (PEO-*b*-PB) polymers. These copolymers form monodisperse nanospheres in dilute deionized water with the aid of 1,4-dioxane as cosolvent (dioxane−H_2O system), while in the THF−H_2O system, some give heterogeneous polydisperse micelles and others form large hollow concentric spherical vesicles ("Russian dolls" arrangement). Smectic stripes inside the vesicles and the nanospheres are clearly visualized by cryo-TEM technique.

Introduction

Recently, the self-assembly behavior of amphiphilic block polymers has attracted more and more attention[1] because the resulting nano- or microsized objects have potential applications in various domains such as material chemistry, drug delivery, biotechnology, etc.[2] We have reported previously several rod−coil amphiphilic block copolymers with liquid crystalline polymers (LCPs) as the hydrophobic rod-like block and PEO (poly(ethylene oxide)) as the hydrophilic coil-like block, which, in dilute aqueous solution, assemble into well organized micro or nanostructures such as spherical vesicles,[3] nanotubes,[4] nanofibers,[5,6] sharp-edged vesicles,[7] and ellipsoidal vesicles.[8] There are several key reasons for the introduction of liquid crystalline elements into the structure of amphiphilic block polymers: (1) Liquid crystal mesogens are densely packed. It might induce an increase of the stiffness of the shells and, as a consequence, a stabilization of the nano-objects. (2) Liquid crystal hydrophobic blocks bring nematic or smectic in-plane order into the hydrophobic blocks. It might be beneficial for the formation of highly ordered nanostructures. Moreover, the in-plane order, competing with the curved geometry of the particles might help to stabilize novel nanostructures with interesting topological defects.[7,8] (3) Using the intrinsic responsive properties of liquid crystalline phases, stimuli-responsive nano-objects could be designed.[9]

In our previous studies, we observed that when the LC hydrophobic blocks presented a smectic mesophase, the self-assembled nano-objects were always nonspherical: fibers,[5,6] sharp-edged[7] vesicles, or ellipsoidal[8] vesicles. These results depart from the usual observations made on the self-assembly of classical amphiphilic block copolymers, for which spherical objects are commonly obtained. All the self-assembly done by us, were performed with amphiphilic block copolymers with PEG hydrophilic groups and LC polyacrylate or methacrylate hydrophobic groups. Could these nonspherical shapes result from a compromise between the highly ordered smectic mesophase and the presence of a "stiff" polymer backbone (polyacrylate or methacrylate)? To try to bring elements of responses to this question, we decided to look for more flexible hydrophobic polymers, such as polybutadiene.

Polymer backbone functionalization method using thiol−ene addition chemistry[10] to graft side-group thiol-containing molecules onto predefined polybutadiene (PB) amphiphilic block copolymers,[11] could be a way to prepare new amphiphilic LC block polymers with a flexible backbone, and study their self-assembly behavior.[12] Compared with the controlled radical polymerization methods we used previously, PB thiol−ene functionalization method has the advantages of easy operation, quick installation and screening of vast amount of side groups to optimize molecular properties for a given application, whereas the main disadvantage is that the resulting functional polymers molecular structures might not be well-defined if the functionalization is not complete.

Ilavsky and Bubnov pioneered in grafting LC mesogens on PB homopolymers[13] and pointed out that polybutadiene, as a very flexible backbone, might theoretically promote tilted smectic phases, but experimentally provided the smectic A phase instead.[13c]

Inspired by the above works, we herein report a series of amphiphilic block copolymers prepared by grafting four different LC mesogens or LC-like side groups on two commercially available PEO-*b*-PB polymers. Depending on the macromolecular structures and preparation conditions, these copolymers self-assemble in water to form monodisperse striped nanospheres or striped hollow concentric spherical vesicles (with a "Russian-dolls" like arrangement).

Experimental Part

Materials and Instrumentation. Two PEO-*block*-PB copolymers (PEO(11500 Da)-*b*-PB(3400 Da), PEO(4000 Da)-*b*-PB(1800 Da))

*Corresponding author. E-mail: patrick.keller@curie.fr.

 Published on Web 12/03/2010

Scheme 1. Functionalization of Two PEO-*b*-PB Copolymers with Four Thiol Compounds

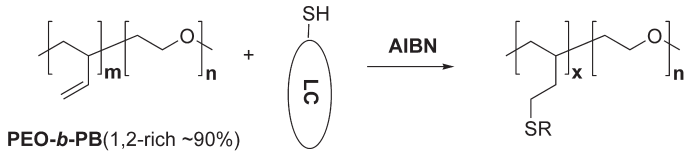

PP1: Vendor reported PEO(11500, MW)-*b*-PB(3400), 1,2-olefin rich ~90%

PP2: Vendor reported PEO(4000, MW)-*b*-PB(1800), 1,2-olefin rich ~90%

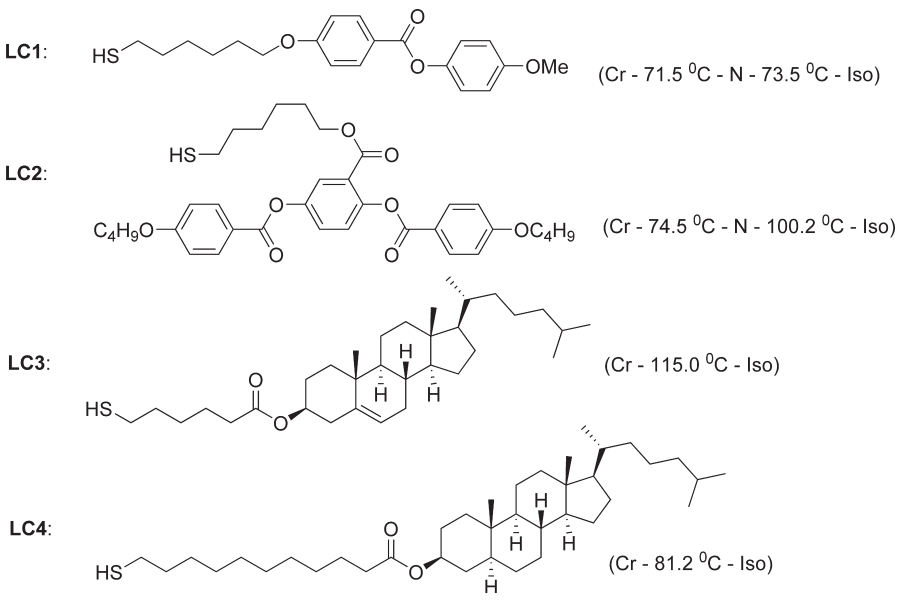

were purchased from Polymer Source Inc. and used as received. 2,2′-Azobis(isobutyronitrile) (AIBN, > 98%, Fluka) and 1-butanethiol (≥99%, Aldrich) were used as received. 1,2-Dichloroethane and dichloromethane were distilled from CaH_2 under argon. THF was distilled from sodium−benzophenone ketyl under argon. 1,4-Dioxane was redistilled under argon.

All ^{1}H NMR spectra were obtained using a Bruker HW300 MHz spectrometer and recorded in $CDCl_3$ (internal reference 7.26 ppm). The molecular weights and the molecular weight distributions of all the polymers were measured by size exclusion chromatography (SEC) using two Waters Styragel HR 5E columns, a Waters 4110 differential refractometer (λ = 930 nm), and a Waters 486 UV detector, in line with a Wyatt miniDAWN light scattering instrument (Ar laser, λ = 690 nm). THF was used as the eluent at 1 mL/min.

The mesomorphic properties were studied by thermal optical polarizing microscopy using a Leitz Ortholux microscope equipped with a Mettler FP82 hot stage and differential scanning calorimetry using a Perkin-Elmer DSC7. The DSC7 was calibrated with Perkin-Elmer indium calibration kit (mp, 429.78 K (156.60 °C); ΔH, 6.80 cal g^{-1}) for temperature and enthalpy changes. The heating and cooling rates were 10 °C/min. X-ray diffraction experiments were performed with a rotating anode generator operated with a small-size focus (copper anode; wavelength λ = 0.15418 nm; focus size, 0.2 × 0.2 mm^2; power, 50 kV, 20 mA).

The morphological analysis of self-assembled aggregates was performed by transmission electron microscopy (TEM) on samples stained by uranyl acetate or by cryogenic transmission electron microscopy (cryo-TEM) on samples fast frozen in liquid ethane. TEM images were recorded using a Philips CM120 electron microscope equipped with a Gatan SSC 1K_1K CCD camera, and the cryo-TEM images were recorded using a Philips CM 120 KV Lab6. Image acquisition and image analysis were performed at the PICT IBISA Imaging Facility.

Synthesis of Thiol-Functionalized Mesogens. Four thiol-functionalized liquid crystalline or liquid crystalline-like compounds were synthesized following the previously published protocol.[14] The detailed experimental procedures and ^{1}H NMR spectra are listed in the Supporting Information.

Synthesis of PEO-*b*-(PB-*g*-LC) Copolymers. Typical procedure: synthesis of block copolymer **PP1-*g*-LC4**. To a solution of 11-Mercapto-undecanoic acid 17-(1,5-dimethylhexyl)-10,13-dimethylhexadecahydrocyclopenta[*a*]phenanthren-3-yl ester, **LC4** (534 mg, 0.91 mmol), and PEO(11500 Da)-*b*-PBD(3400 Da) (71.5 mg, 0.0048 mmol) in 0.91 mL of 1,2-dichloroethane in a pressure tube, was added AIBN (22.2 mg, 0.13 mmol) under argon. The reaction mixture was degassed and exchanged with argon via three freeze−thaw cycles, sealed, and heated to 65 °C in an oil bath for 48 h. After cooling down, the polymer was precipitated from the solution by addition of a large amount of diethyl ether, and separated by centrifugation. This precipitation−centrifugation step was repeated several times, finally providing the corresponding polymer as a white powder (135 mg).

Self-Assembly of the Amphiphilic Block Copolymers in Water. The block copolymers were first dissolved in 1,4-dioxane or THF, at a concentration of 1.0 mg/mL. Deionized water was then added very slowly (5 μL portions) into 1.0 mL of the solution under gentle shaking. After each addition of water droplet, the solution was left to equilibrate for 5 min. The cycles of water addition and equilibration were stopped after a total amount of 1.5 mL water has been added. The turbid solution was then dialyzed against deionized water (water changed every 6 h) for 3 days to remove all the organic solvents, using a Spectra/Por regenerated cellulose membrane with a molar mass cutoff of 3500 Da.

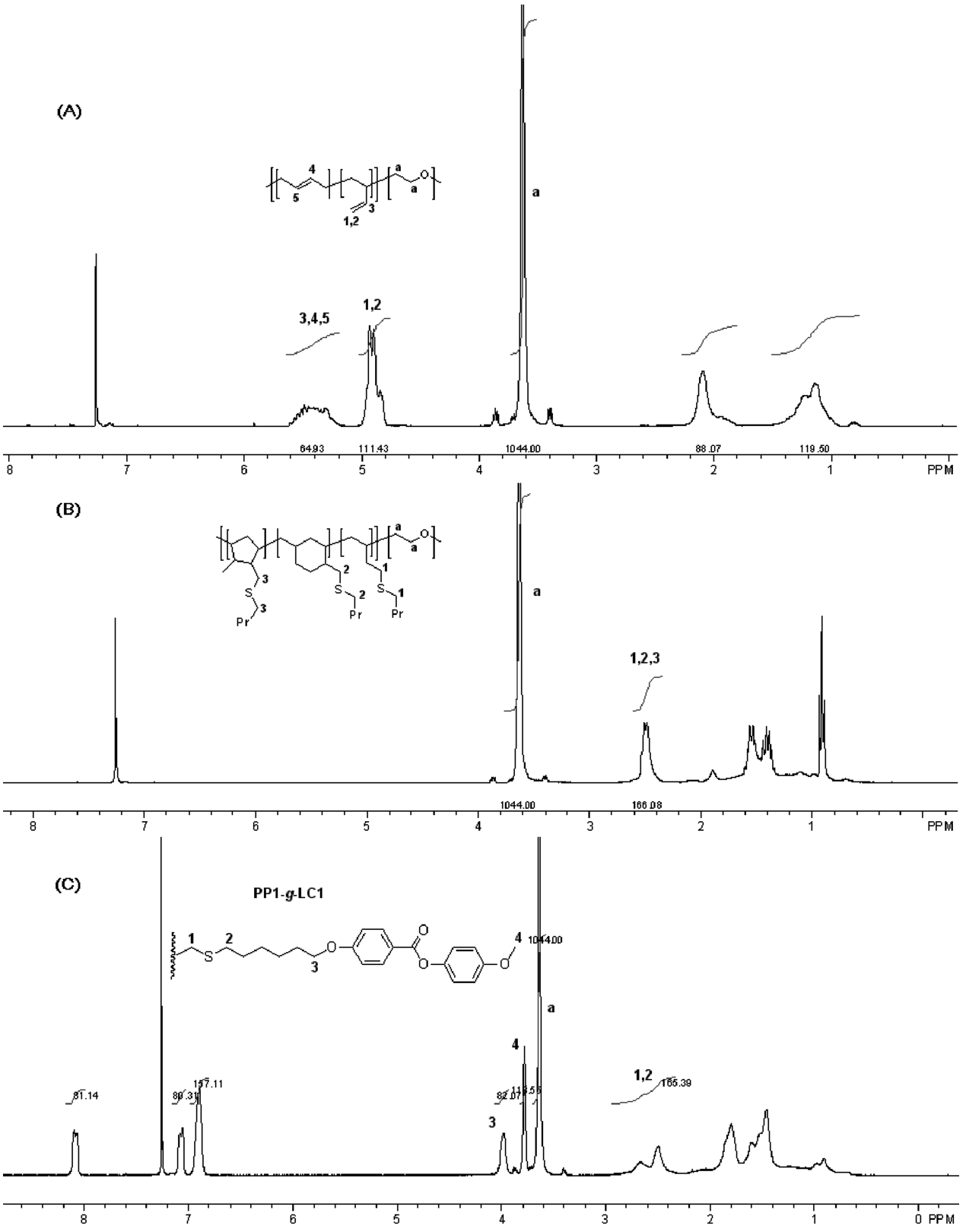

Figure 1. ^{1}H NMR spectra of (A) PP1, (B) PP1-*g*-Bu, and (C) PP1-*g*-LC1.

Results and Discussion

Synthesis and Characterization of Amphiphilic Block Copolymers. As shown in Scheme 1, two PEO-*b*-PB polymers (PEO(11500 Da)-*b*-PB(3400 Da), PEO(4000 Da)-*b*-PB(1800 Da)) were purchased from Polymer Source Inc. Assuming the molecular weights of the PEO blocks were authentic, we used NMR experiments (Figure 1A) to calculate the degrees of polymerization (DP) of the PB blocks, and finally obtained the following compositions for the two PEO-*b*-PB copolymers: **PP1**, PEO(261, DP)-*b*-PB(60.3 total DP, 1,2-olefin 55.7; 1,4-olefin 4.6) and **PP2**, PEO(90, DP)-*b*-PB(29.9 total DP, 1,2-olefin 28.2; 1,4-olefin 1.7).

Scheme 2. Possible Reaction Routes for 1,4-Olefin in Polybutadiene Backbone

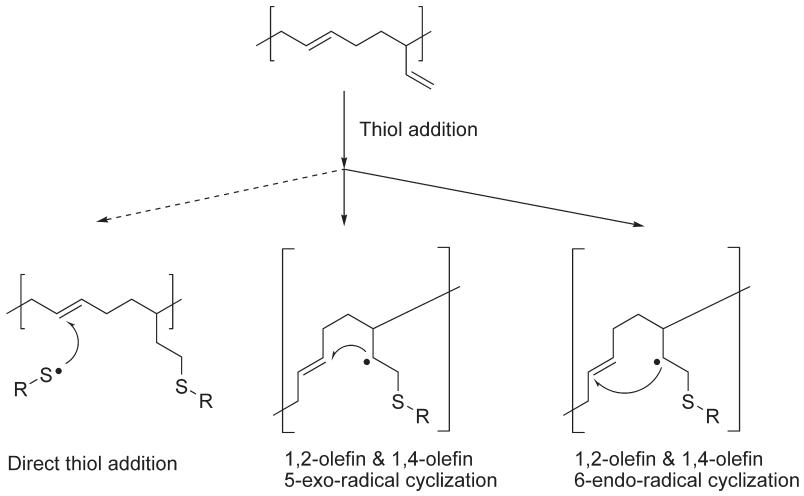

Three side-end and one side-on thiol mesogenic molecules (Scheme 1) were synthesized (details of synthetic protocols and NMR spectra are presented in the Supporting Information). On the basis of our experience, **LC1**, **LC2** and **LC3,** which have molecular structures similar to previously published examples,[3−8] might bring smectic or nematic mesomorphic order into the corresponding copolymers. **LC4,** a (2H)-cholesteryl derivative, has a new molecular structure, designed to exclude a possible thiol−ene side reaction which could take place between the carbon−carbon double bond of a regular cholesteryl derivative and a thiol function. **LC1** and **LC2** exhibit mesophases, while **LC3** and **LC4** show a direct crystalline-isotropic phase transition. The transition temperatures (Scheme 1) were determined by polarized optical microscopy.

In order to get block copolymers with a mesomorphic hydrophobic block, as many LC mercaptans as possible had to be grafted onto the PB backbone. It is now well-established that PB chains with very high 1,2-olefin content submitted to thiol−ene reaction conditions, tend to form cyclic adducts (five-member rings or six-member rings), which, usually, limit the functionalization to ≤50%,[11,15] while, in some very specific conditions, very high thiol concentrations could afford up to 70−85% functionalization,[11b,c] (however, a full functionalization has never been reported so far). In a limited approach to find "optimized" functionalization conditions for our specific PEO-*b*-PB copolymers, we tested the PB functionalization at the highest concentration possible in thiol functions, using butanethiol as both reactant and solvent.

Using the methylene protons of the PEO block as the integration reference, PB functionalization calculations based on ^{1}H NMR analysis were quite reliable. As shown in Figure 1B, the aliphatic protons of chemical shifts around 2.5 ppm all belong to R**CH_2SCH_2**−, which stands on an assumption that 1,4-olefins could only participate in cyclization reactions but not in direct thiol addition reactions (Scheme 2) otherwise the coexistence of R**CH_2SCH**− would complicate the functionalization calculation. There are two evidence supporting this assumption: (1) 1,2-olefins have a much higher kinetic constant in thiol−ene additions with respect to 1,4-units;[16] (2) our later PEO-*b*-(PB-*g*-LCs) results support this assumption. For example, as shown in Figure 1C, the integration value of R**CH_2SCH_2**- protons of chemical shifts around 2.5 ppm is exactly twice of the one of −**CH_2O**− around 4.0 ppm, and all the olefins (chemical shifts 4.8−5.6 ppm) have disappeared.

Many factors, like the fine structures of PB polymers, reaction temperatures, solvents, thiol reactants, radical initiators, and concentrations of all reagents, could affect the PB functionalization. In our experiments, we set all the reaction temperatures to 65 °C and only studied the PB functionalization by changing the concentrations of thiol compounds and of radical initiator, AIBN. Using *n*-butanethiol as the reactant and the solvent, the thiol concentration was the highest possible (9.28 mol/L). Herein, we define the initial molar concentration of all PB double bond units, $[C{=}C]_0$ = DP * $[PB]_0$, where DP is the degree polymerization of PB, and $[PB]_0$ is the initial molar concentration of PB polymer. When the molar ratio of AIBN to all PB double bond units was much lower than 1 or higher than 1 (Table1, entry 3−4), the PB thiol−ene functionalization resulted in a constant 69%, which means the concentration and molar ratio of AIBN do not strongly affect the PB functionalization.

Next, thiol-functionalized LC molecules were grafted onto **PP1** copolymer. When the mercaptan had a very low initial concentration of 0.05 mol/L, with one equivalent mole of all PB double bond units used, the PB functionalization was only 23% (Table 1, entry 5). When the initial thiol concentration was increased to 0.10 mol/L and three equivalent moles of all PB double bond units were used, the PB functionalization increased to 42%, while there was still some trace amount of double bonds remaining unreacted on the PB backbone (Table 1, entry 6). When the initial thiol concentration was increased to 1.00 mol/L and three equivalent moles of all PB double bond units were used, 66%-69% PB functionalization was achieved for all the copolymers (Table 1, entry 7−10), and all the olefins of PB were consumed. Interestingly, when the same reaction conditions were applied to graft **LC4** onto a shorter copolymer **PP2**, PB functionalization was still around 69%. (Table 1, entry 11)

Mesomorphic Properties of the Amphiphilic Block Copolymers. The mesomorphic properties of these amphiphilic block copolymers were studied by polarized optical microscopy (POM), DSC and X-ray diffraction techniques. By POM, the liquid crystalline blocks show the phase transitions as follow (observed on heating): **PP1-*g*-LC1**, Cr−59 °C−SmX−90 °C−Iso; **PP1-*g*-LC2**, Cr−56 °C−N−80 °C−Iso; **PP1-*g*-LC3**, Cr−85 °C−Iso; **PP1-*g*-LC4**, Cr−55 °C−SmX−108 °C−Iso; **PP2-*g*-LC4**, Cr−51 °C−SmX−106 °C−Iso. Above the LC blocks isotropic temperatures, weak birefringence remained for all block copolymers, which might be a signature of a lamellar order resulting from the incompatibility between the PEO and LC blocks. Typical photos of textures obtained

Table 1. Reaction Conditions and Characterization of PEO-*b*-PB Polymers[i]

entry	polymers	$[RSH]_0$[b] (mol/L)	$[RSH]_0/[C{=}C]_0$[c]	$[AIBN]_0/[C{=}C]_0$[c]	f[d]	M_n[e](Da)	M_w/M_n	R[f]	mesophase[g]
1	**PP1**					20 130	1.05	78/22	no
2	**PP2**					20 720	1.05	71/29	no
3[a]	**PP1-*g*-Bu**	9.28	> 100	0.15	0.69[h]	20 110	1.10	62/38	no
4[a]	**PP1-*g*-Bu**	9.28	> 100	1.50	0.69[h]	20 050	1.10	62/38	no
5	**PP1-*g*-LC1**	0.05	1.00	0.15	0.23	12 480	1.20	58/42	no
6	**PP1-*g*-LC3**	0.10	3.00	0.15	0.42	15 530	1.17	41/59	no
7	**PP1-*g*-LC1**	1.00	3.00	0.15	0.68[h]	13 800	1.22	39/61	smectic
8	**PP1-*g*-LC2**	1.00	3.00	0.15	0.67[h]	15 040	1.16	29/71	nematic
9	**PP1-*g*-LC3**	1.00	3.00	0.15	0.66[h]	19 970	1.18	33/67	no
10	**PP1-*g*-LC4**	1.00	3.00	0.15	0.69[h]	24 460	1.11	29/71	smectic
11	**PP2-*g*-LC4**	1.00	3.00	0.15	0.69[h]	17 650	1.07	23/77	smectic

[a] Neat reactions using *n*-butanethiol as the reactant and solvent. [b] The volumes of LC mercaptans, polymers and AIBN are neglected. [c] In molar equivalents of PB double bonds. [d] *f* represents the degree of functionalization, determined by ^{1}H NMR. [e] Molecular weight measurements were analyzed based on calibration using polystyrene standards. [f] R represents the ratio of hydrophilic block weight/Hydrophobic block weight. [g] Mesophases are determined by polarized microscope observation. [h] All olefins were consumed. [i] Note: All reactions were carried out in 1,2-dichloroethane at 65 °C for 48 h.

Scheme 3. Previously Published Smectic Amphiphilic Block Copolymers Molecular Structures and Smectic Layer Distances Measured by SAXS and cryo-TEM

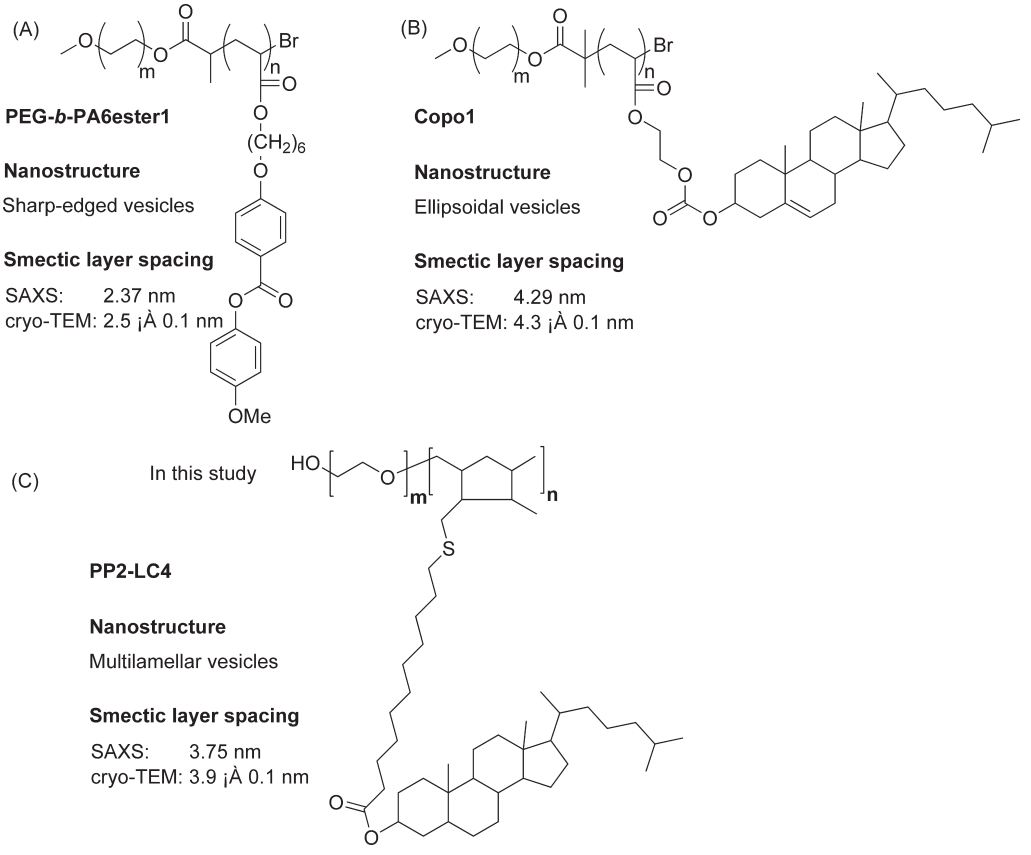

for the LC block copolymers and the DSC spectra of these block copolymers are presented in the Supporting Information. A series of X-ray diffraction experiments on some of the copolymers samples were also carried out at room temperature to confirm the identification of the mesophases, and are reported in the Supporting Information.

PP1-*g*-LC1 smectic order and **PP1-*g*-LC2** nematic order are consistent with our previous reports.[4,7] Surprisingly, **PP1-*g*-LC3**, which possesses a molecular structure similar to the smectic copolymer **Copo1** (Scheme 3B),[8] shows no mesophase. One possible reason might be found in the complicated structure of the PB backbone after grafting, needing longer spacers to allow the cholesteryl groups to arrange into liquid crystalline organization. Accordingly, **PP1-*g*-LC4** and **PP2-*g*-LC4**, with much longer C_{10} alkyl spacers, presents mesomorphic properties.

Smectic order in **PP2-*g*-LC4** was confirmed by the X-ray diffraction data given in Figure 2. The layer spacing of this block copolymer is almost constant over a wide temperature range of 20−95 °C (see Figure 2A), while no layer was observed above 105 °C which is the clearing point. Figure 2B shows the small-angle X-ray scattering (SAXS) pattern of **PP2-*g*-LC4** at room temperature; the smectic layer spacing associated with the Bragg reflections is $p = 3.75$ nm. Comparing with PAChol layer spacing in **Copo1**[8] (4.29 nm, see Scheme 3B), the layer spacing for **LC4** (3.75 nm) is much smaller, although **PP2-*g*-LC4** has a much longer flexible spacer than **Copo1** (15 atoms linking instead of 7 atoms linking between the polymer backbone and the cholesteryl group). The 4.29 nm period in **Copo1** corresponds to a value between l and $2l$, $l = 2.65$ nm being the fully extended length of the cholesteryl mesogen, as estimated by Dreiding models. The smectic

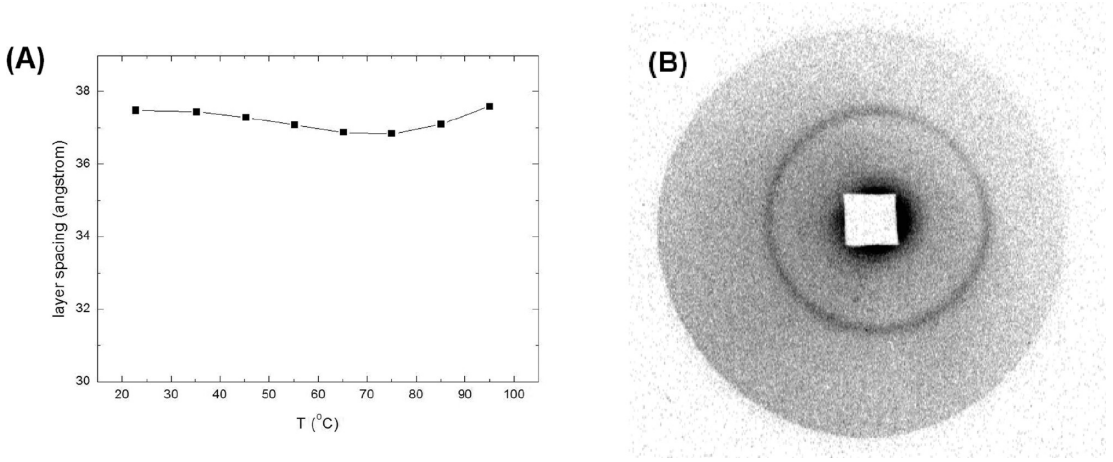

Figure 2. (A) X-ray diffraction results showing the observed layer spacing of **PP2-*g*-LC4** at 20−95 °C temperature range. (B) SAXS pattern of **PP2-*g*-LC4** at room temperature.

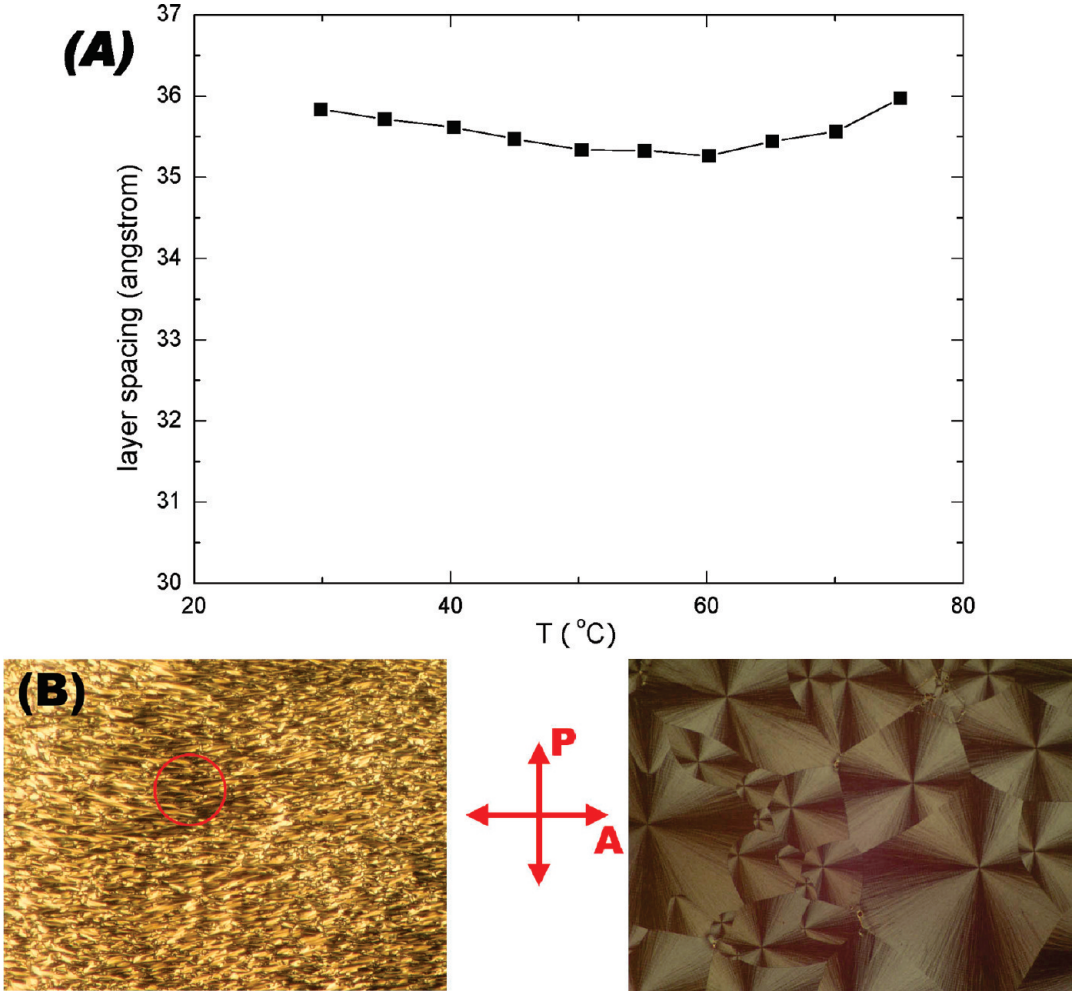

Figure 3. (A) X-ray diffraction results showing the observed layer spacing of **PB-*g*-LC4** at 25−75 °C temperature range. (B) POM images of **PB-*g*-LC4** at 50 °C (left) and 25 °C (right).

mesophase is an interdigitated two-layer smectic A phase (SmA_d) with the side groups overlapping in the tails region.[8] The LC4 block in **PP2-*g*-LC4** might possess a SmA phase with a one-layer antiparallel packing, since the smectic period (3.75 nm) is close to the extended mesogen length l = 4.60 nm. The difference might come from the coiled conformation of the aliphatic spacer.[17] Alternatively, the smectic mesophase could be a tilted smectic phase (SmC) with one laying antiparallel packing of the side group.

In order to determine more precisely the nature of the smectic mesophase of **PP2-*g*-LC4**, we tried to align this sample, which however failed since the PEG block greatly increased the viscosity of this copolymer and consequently complicated the mesophase observation. The alternative option was to study instead the mesophase of **PB-*g*-LC4** homopolymer

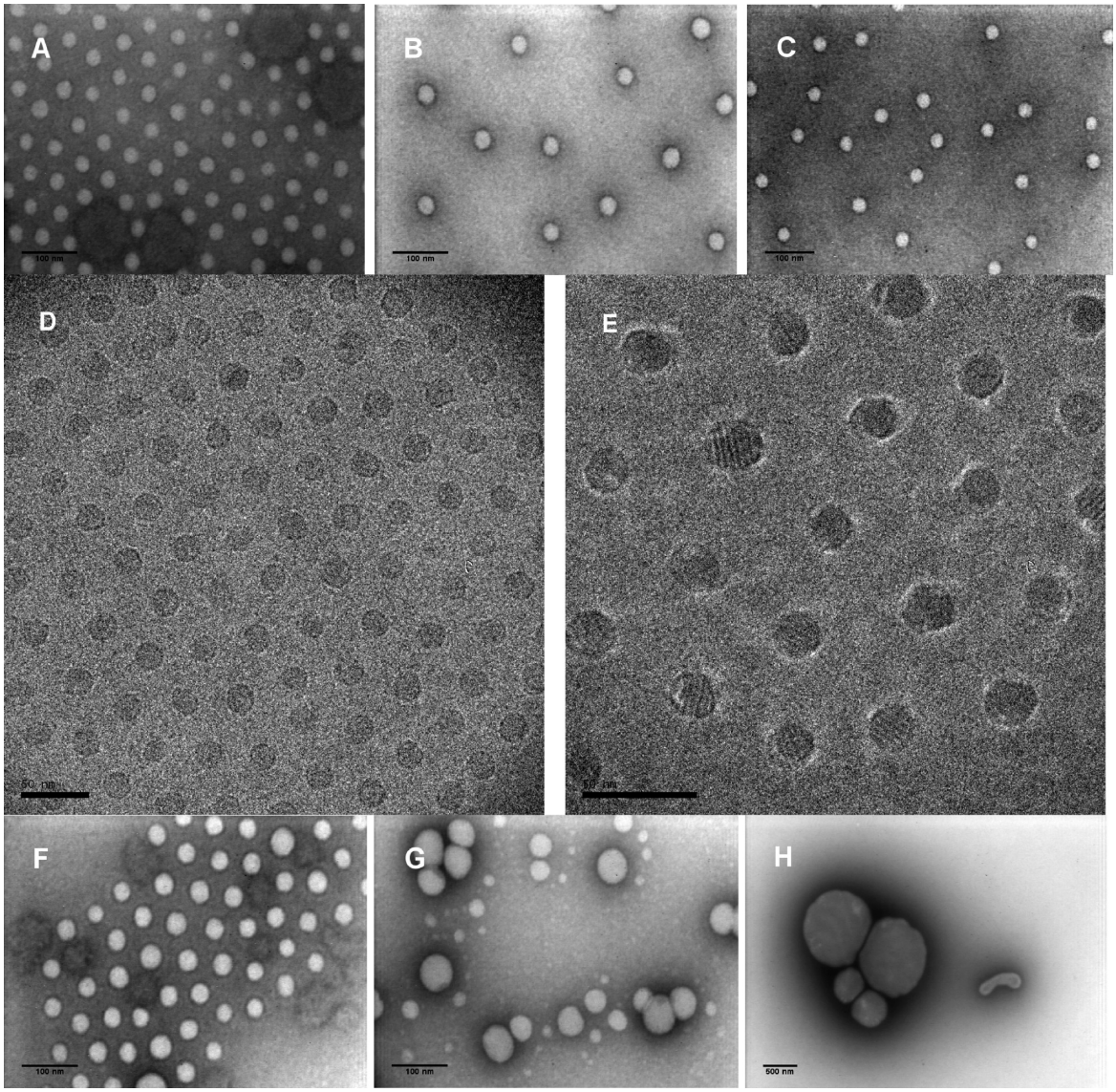

Figure 4. TEM images of block copolymer self-assemblies. In 1,4-dioxane−H_2O system: **PP1-*g*-LC1** (A), **PP1-*g*-LC2** (B), and **PP1-*g*-LC3** (C). In THF − H_2O system: **PP1-*g*-LC1** (F), **PP1-*g*-LC2** (G), and **PP1-*g*-LC3** (H). (D) and (E) show cryo-TEM images of **PP1-*g*-LC1** block copolymer self-assemblies in 1,4-dioxane−H_2O system. (A−C, F−H, scale bar = 100 nm; D, E, scale bar = 50 nm.).

which should have similar smectic arrangements as **PEG-*b*-PB-*g*-LC4** and much lower viscosity for alignment. **PB-*g*-LC4** was synthesized by grafting LC4 on a commercially available polybutadiene (M.W. 3000 Da, 1,2-olefin >90%, Aldrich Inc.). By POM and DSC (see the Supporting Information), the corresponding phase transitions are the followings: Cr−35 °C−SmX−71 °C−Iso (observed on heating). The layer spacing of this homopolymer is very similar to the one of **PP2-*g*-LC4** block copolymer (Figure 3A), which could be a solid proof for them to both have identical smectic arrangement. The homopolymer sample was then introduced by capillarity at a temperature above its clearing point, into a 5 μm thick cell with both surfaces pretreated with polyimide and rubbed unidirectionally. When the cell was cooled to 50 °C, the POM image showed a SmA texture with the so-called bâtonnets.[18] As shown in Figure 3B, the layer normal is along the fast growth direction of bâtonnets, i.e. horizontal in the marked region. When bâtonnets are rotated to the analyzer direction (horizontal in the marked circle region), they look dark, suggesting the optic axis is along the smectic layer normal, thus it is a Smectic A phase. A crystal phase appears at lower temperature with much lower birefringence; interestingly, it shows four dark brushes, with the brush directions along the polarizer and analyzer. On the basis of all the above experiments, we can conclude that **PP2-*g*-LC4** has a SmA arrangement, which is in fact consistent with Bubnov's observations on **PB-*g*-LC** homopolymers.[13]

Self-Assembly Behavior of the Amphiphilic Block Copolymers in Water. Self-assembly of PEO-*b*-(PB-*g*-LC) copolymers in dilute aqueous solution was performed with the aid of organic solvents. 1,4-Dioxane and THF were used in this study. The morphologies of all the observed nano-objects are summarized in Table 2.

As shown in Figure 4A-C, analysis by TEM with negative staining revealed that **PP1-*g*-LC1** (**39/61, hydrophilic/hydrophobic weight ratio**), **PP1-*g*-LC2** (**29/71**), and **PP1-*g*-LC3** (**33/67**) all form very uniform nanospheres with diameters around 28 ± 1 nm when self-assembled in dioxane-H_2O system. Cryo-TEM was used to study the fine structure of **PP1-*g*-LC1** nanospheres (Figure 4D-E), which show stripes with a periodic spacing of 2.9 ± 0.1 nm inside these objects. These stripes are the signature of the smectic order present in the hydrophobic blocks of the diblock copolymer, as developed in our previous works.[5,7,8] For example, **PEG-*b*-PA6ester1**

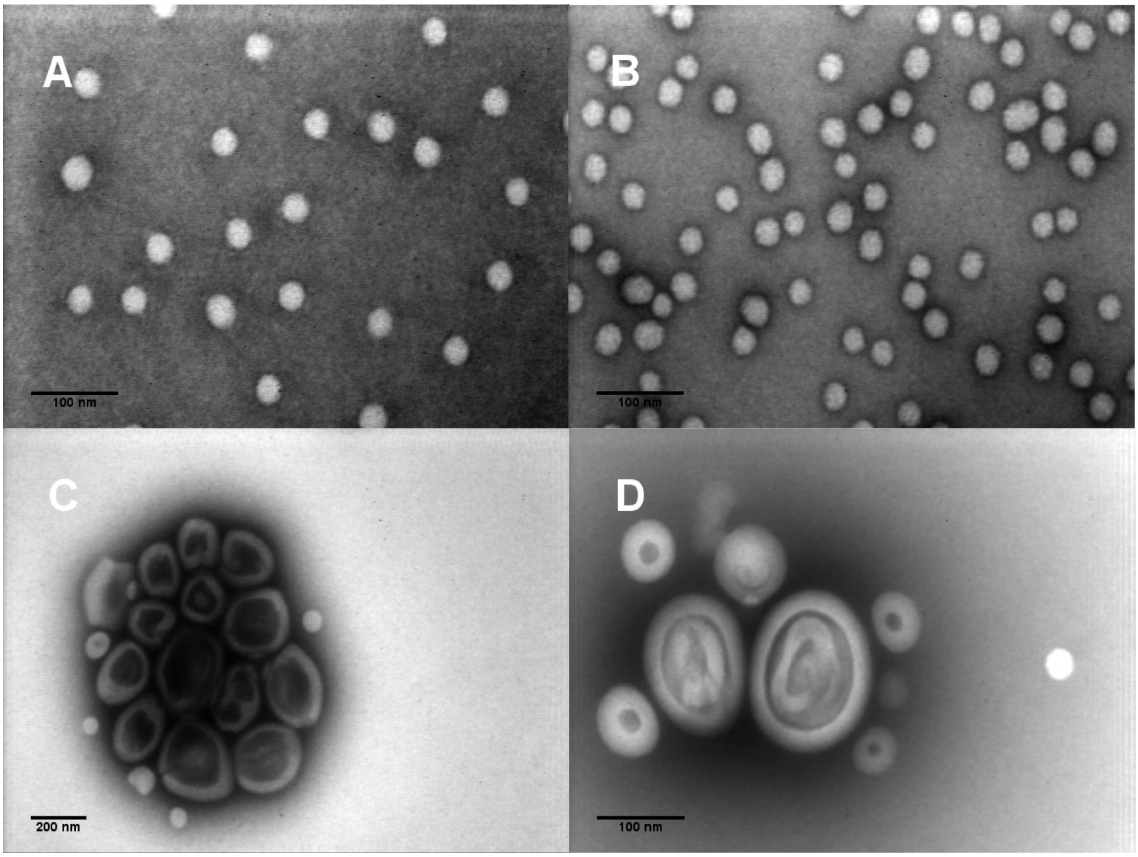

Figure 5. TEM images of PP1-*g*-LC4 and PP2-*g*-LC4 block copolymers self-assemblies in 1,4-dioxane−H_2O system (A, B) and in THF−H_2O system (C, D). (A, B, D, scale bar = 100 nm; C, scale bar = 200 nm.).

Table 2. Morphologies of all the Self-Assembled PEO-*b*-(PB-*g*-LC) Polymers Nano-Objects in 1,4-Dioxane−H_2O and THF−H_2O Systems

	morphologies of self-assembled nano-objects	
copolymers	in dioxane−H_2O	in THF−H_2O
PP1-*g*-LC1	monodisperse nanospheres	nanospheres
PP1-*g*-LC2	monodisperse nanospheres	ill-determined aggregates
PP1-*g*-LC3	monodisperse nanospheres	ill-determined aggregates
PP1-*g*-LC4	monodisperse nanospheres	polydisperse spherical vesicles
PP2-*g*-LC4	monodisperse nanospheres	polydisperse spherical vesicles

(Scheme 3A), with a side group molecular structure similar to the one found in **PP1-*g*-LC1** showed smectic stripes on the membrane surfaces of the self-assembled sharp-edged vesicles.[7] Since the PEO corona of block copolymer micelles is usually invisible by cryo-TEM because of its low electron density and low contrast,[19] the PB-*g*-LC core diameter and the total diameter can be measured respectively from TEM and cryo-TEM micrographs: $D_{core} = 20 \pm 1$ nm, $D_{total} = 28 \pm 1$ nm. Meanwhile, the well-defined micelle core sizes determined by TEM (Figure 3D,E) allow the calculation of the aggregation number,[20] N_{agg} given by

$$N_{agg} = (4/3)\pi {R_{core}}^3 / V_{PB\text{-}g\text{-}LC} \quad (1)$$

where R_{core} is the PB-*g*-LC core radius, $V_{PB\text{-}g\text{-}LC}$ is the volume per PB-*g*-LC block chain. Assuming the density of PB-*g*-LC blocks is close to 1, N_{agg} could thus be estimated as around 140−150.

In THF−H_2O system (Figure 4F−H), **PP1-*g*-LC1** forms also nanospheres which are not very uniform, while **PP1-*g*-LC2** and **PP1-*g*-LC3** form ill-determined aggregates with larger sizes.

Here, all the polymers discussed so far formed spherical micelles in dioxane−H_2O, in contrast with the vesicles formed by other copolymers with similar hydrophilic/hydrophobic weight ratios in our previous works.[3,4,7,8] This difference could be related to the presence of very long hydrophilic blocks for these copolymers (MW = 11500 Da for PP1 and MW = 4000 Da for PP2), as compared with the previous works (MW = 2000 Da). The spherical micelles might be more easily stabilized by the long PEO chains.

PP1-*g*-LC4 (**29/71**) and **PP2-*g*-LC4** (**23/77**) both form nanospheres with narrow size distribution (25−30 nm in diameter) (Figure 5A,B) in dioxane−H_2O system. However, when self-assembled in THF-H_2O system, **PP1-*g*-LC4** (**29/71**) and **PP2-*g*-LC4** (**23/77**) both formed vesicles with diameters ranging from 50 to 200 nm (Figure 5C,D). Cryo-TEM was used to study the fine structure of **PP2-*g*-LC4** vesicles. Three types of vesicles were observed (Figure 6): unilamellar spherical vesicles (25−50 nm in diameter), hollow concentric spherical vesicles with a "Russian dolls like" arrangement (150−200 nm in diameter for the largest external ones), "broken" concentric spherical vesicles (150−200 nm in diameter). The thickness of the vesicles membrane is rather uniform, $d = 13.7 \pm 0.1$ nm. Moreover, a careful analysis of the vesicles formed by **PP2-*g*-LC4** revealed a striped structure in some parts of the membranes. The period, calculated by Fourier

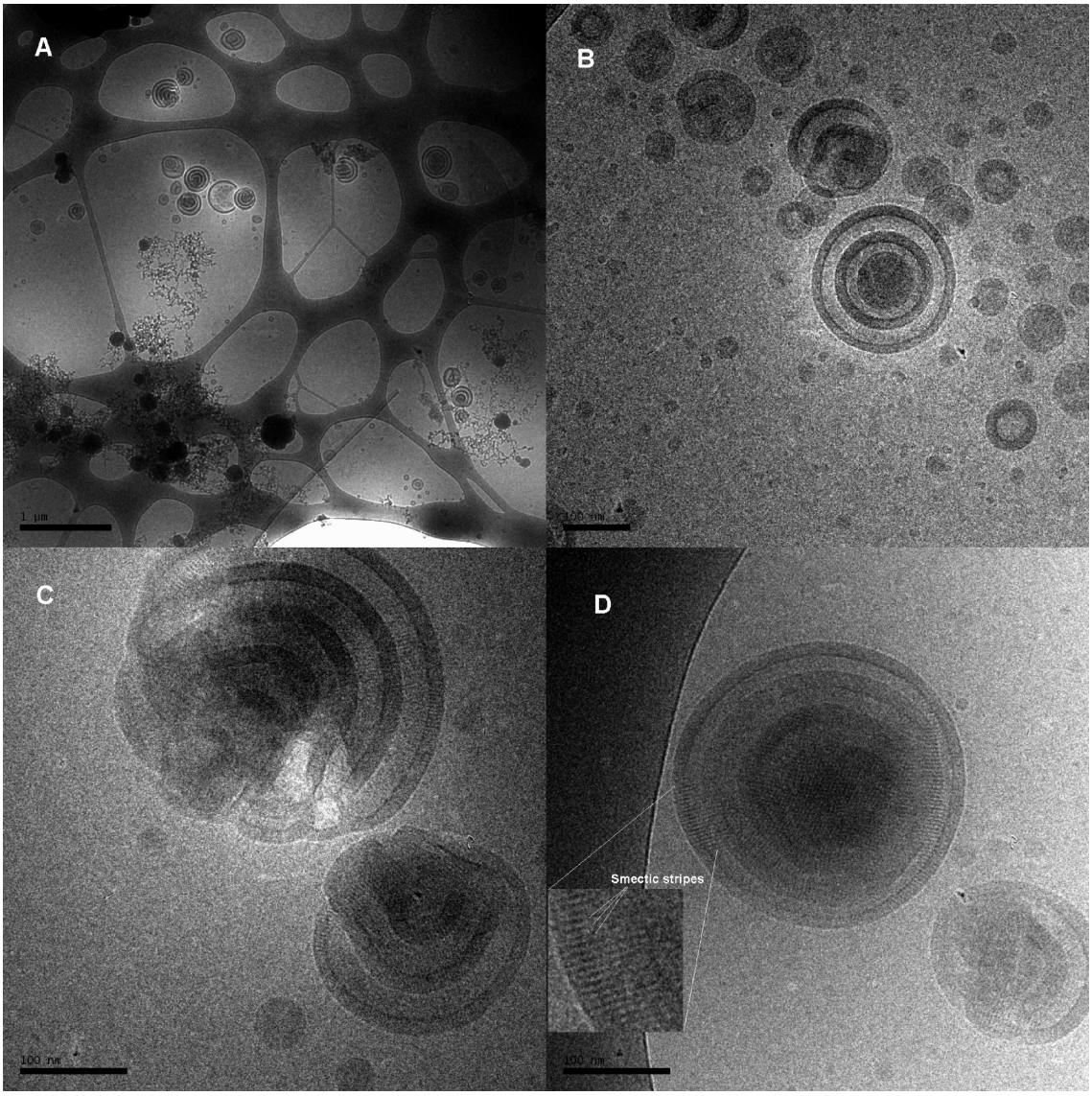

Figure 6. cryo-TEM images of **PP2-*g*-LC4** block copolymer self-assembly in the THF−H_2O system (A, scale bar = 1000 nm; B−D, scale bar = 100 nm).

transform of the cryo-TEM image,[7] is of 3.9 ± 0.1 nm, in agreement with the SAXS measurements discussed above. These stripes reveal the smectic organization of the mesogens in the 2D membrane.

Up to now, self-assembly in water of PEO-*b*-smectic polymers had produced, among other aggregates, "faceted" or "ellipsoidal" unilamellar striped vesicles.[7,8] On the other hand, hollow concentric vesicles have been found for classical amphiphilic block copolymers such as PS-*b*-PAA, PEO-*b*-PBA and PEO-*b*-PBO.[21−24] One of the remarkable features for **PP2-*g*-LC4** self-assembly in water is the existence of "striped" hollow concentric spherical vesicles. At this stage, it is difficult to build up a realistic scenario explaining the formation of those unique aggregates. The shape and structure of the aggregates result from a subtle balance between different properties such as the hydrophilic−hydrophobic diblock composition, the flexibility of the polymer backbones, the rigidity of the smectic membrane, the quality of the organic solvent used in the preparation, etc. The pronounced flexibility of PB backbone as compared to polyacrylate backbone, and its incomplete functionalization by the mesogenic side groups (only 69% substitution), might confer to the membrane the flexibility needed to give the vesicle the possibility to adopt a spherical shape. In order to better understand what parameters govern these morphologies, further experiments are needed, including the synthesis of new diblock copolymers with diversified macromolecular backbones and/or mesogenic groups.

Conclusion

In the current study, we observed novel striped hollow concentric spherical vesicles ("Russian dolls" organization) possessing smectic order inside the hydrophobic shells by self-assembly of poly(ethylene oxide)-*block*-(polybutadiene-*graft*-liquid crystal) in water. To prepare these new amphiphilic block copolymers, we successfully applied a "thiol−ene" radical addition reaction to graft several liquid crystalline mesogens on amphiphilic poly(ethylene oxide)-*block*-polybutadiene copolymers.

It is the first time we observed spherical arrangements in amphiphilic block copolymers possessing smectic order inside the hydrophobic blocks using polybutadiene as the polymer backbones. The spherical vesicle morphology, not found in other vesicles with a smectic hydrophobic block containing a stiff acrylate backbone, might be related to the competition between the high flexibility of hydrophobic backbone and the liquid crystalline orientational/positional order.

Acknowledgment. We thank the Agence Nationale de la Recherche (award *N*° ANR-07-MAPR-0020-02), and National Natural Science Foundation of China (Grant No. 21002012) for financial support of this work and The Curie Institute Research Center for a fellowship (to H.Y.). We also greatly thank Dr. Ren-Fan Shao for fruitful discussions about LC mesophase identification.

Supporting Information Available: Text giving experimental details on the synthesis of the mercaptans and block copolymers, as well as characterization of their mesomorphic properties (DSC, POM and X ray diffraction). This material is available free of charge via the Internet at http://pubs.acs.org.

References and Notes

(1) (a) Discher, D. E.; Eisenberg, A. *Science* **2002**, *297*, 967–973. (b) Kita-Tokarczyk, K.; Grumelard, J.; Haefele, T.; Meier, W. *Polymer* **2005**, *46*, 3540–3563. (c) Kukula, H.; Schlaad, H.; Antonietti, M.; Forster, S. *J. Am. Chem. Soc.* **2002**, *124*, 1658–1663. (d) Riess, G. *Prog. Polym. Sci.* **2003**, 1107–1170.

(2) (a) York, A. W.; Kirkland, S. E.; McCormick, C. L. *Adv. Drug Delivery Rev.* **2008**, 1018–1036. (b) Discher, D. E.; Ortiz, V.; Srinivas, G.; Klein, M. L.; Kim, Y.; Christian, D.; Cai, S.; Photos, P.; Ahmed, F. *Prog. Polym. Sci.* **2007**, *32*, 838–857. (c) Taubert, A.; Napoli, A.; Meier, W. *Curr. Opin. Chem. Biol.* **2004**, *8*, 598–603. (d) Joralemon, M. J.; McRae, S.; Emrick, T. *Chem. Commun.* **2010**, *46*, 1377–1393.

(3) Yang, J.; Levy, D.; Deng, W.; Keller, P.; Li, M.-H. *Chem. Commun.* **2005**, 4345–4347.

(4) Yang, J.; Pinol, R.; Gubellini, F.; Levy, D.; Albouy, P.-A.; Keller, P.; Li, M.-H. *Langmuir* **2006**, *22*, 7907–7911.

(5) Pinol, R.; Jia, L.; Gubellini, F.; Levy, D.; Albouy, P.-A.; Keller, P.; Cao, A.; Li, M.-H. *Macromolecules* **2007**, *40*, 5625–5627.

(6) Boisse, S.; Rieger, J.; Di-Cicco, A.; Albouy, P.-A.; Bui, C.; Li, M.-H.; Charleux, B. *Macromolecules* **2009**, *42*, 8688–8696.

(7) Xu, B.; Pinol, R.; Nono-Djamen, M.; Pensec, S.; Keller, P.; Albouy, P.-A.; Levy, D.; Li, M.-H. *Faraday Discuss.* **2009**, *143*, 235–250.

(8) Jia, L.; Cao, A.; Levy, D.; Xu, B.; Albouy, P.-A.; Xing, X.; Bowick, M. J.; Li, M.-H. *Soft Matter* **2009**, *5*, 3446–3451.

(9) Mabrouk, E.; Cuvelier, D.; Brochard-Wyart, F.; Nassoy, P.; Li, M.-H. *Proc. Natl. Acad. Sci. U.S.A.* **2009**, *106*, 7294–7298.

(10) See a review: Kade, M. J.; Burke, D. J.; Hawker, C. J. *J. Polym. Sci., Part A: Polym. Chem.* **2010**, *48*, 743–750.

(11) (a) Justynska, J.; Schlaad, H. *Macromol. Rapid Commun.* **2004**, *25*, 1478–1481. (b) Justynska, J.; Hordyjewicz, Z.; Schlaad, H. *Polymer* **2005**, *46*, 12057–12064. (c) Justynska, J.; Hordyjewicz, Z.; Schlaad, H. *Macromol. Symp.* **2006**, *240*, 41–46. (d) Brummelhuis, N. T.; Diehl, C.; Schlaad, H. *Macromolecules* **2008**, *41*, 9946–9947.

(12) (a) You, L.; Schlaad, H. *J. Am. Chem. Soc.* **2006**, *128*, 13336–13337. (b) Geng, Y.; Discher, D. E.; Justynska, J.; Schlaad, H. *Angew. Chem., Int. Ed.* **2006**, *45*, 7578–7581. (c) Voets, I. K.; Keizer, A. D.; Stuart, M. A. C.; Justynska, J.; Schlaad, H. *Macromolecules* **2007**, *40*, 2158–2164. (d) Hordyjewicz-Baran, Z.; You, L.; Smarsly, B.; Sigel, R.; Schlaad, H. *Macromolecules* **2007**, *40*, 3901–3903. (e) Sigel, R.; Losik, M.; Schlaad, H. *Langmuir* **2007**, *23*, 7196–7199. (f) Konak, C.; Subr, V.; Kostka, L.; Stepanek, P.; Ulbrich, K.; Schlaad, H. *Langmuir* **2008**, *24*, 7092–7098.

(13) (a) Jigounov, A.; Sedlakova, Z.; Spevacek, J.; Ilavsky, M. *Eur. Polym. J.* **2006**, *42*, 2450–2457. (b) Bubnov, A.; Kaspar, M.; Sedlakova, Z.; Ilavsky, M. *Liq. Cryst.* **2008**, *35*, 653–660. (c) Kaspar, M.; Bubnov, A.; Sedlakova, Z.; Stojanovic, M.; Havlicek, J.; Obadaovic, D. Z.; Ilavsky, M. *Eur. Polym. J.* **2008**, *44*, 233–243.

(14) (a) Yang, H.; Buguin, A.; Taulemesse, J. M.; Kaneko, K.; Mery, S.; Bergeret, A.; Keller, P. *J. Am. Chem. Soc.* **2009**, *131*, 15000–15004. (b) Yang, H.; Wang, L.; Shao, R.; Clark, N. A.; Ortega, J.; Etxebarria, J.; Albouy, P. A.; Walba, D. M.; Keller, P. *J. Mater. Chem.* **2009**, *19*, 7208–7215. (c) Yang, H.; Richardson, J.; Walba, D. M.; Zhu, C.; Shao, R. F.; Clark, N. A.; Ortega, J.; Etxebarria, J.; Keller, P. *Liq. Cryst.* **2010**, *37*, 325–334.

(15) David, R. L. A.; Kornfield, J. A. *Macromolecules* **2008**, *41*, 1151–1161.

(16) (a) Schapman, F.; Youseff, B.; About-Jaudet, E.; Bunell, C. *Polymer* **1998**, *39*, 4955–4962. (b) Lotti, L.; Coiai, S.; Ciardelli, F.; Galimberti, M.; Passagalia, E. *Macromol. Chem. Phys.* **2009**, *210*, 1471–1483.

(17) Shibaev, V. P.; Platé, N. A. In *Advances in Polymer Science 60/61: Liquid Crystal Polymers II/III*; Springer-Verlag: Berlin, 1984; pp 175−252.

(18) Dierking, I. *Textures of Liquid Crystals*; Wiley-VCH: Weinheim, Germany, 2003.

(19) Mortensen, K.; Talmon, Y.; Gao, B.; Kops, J. *Macromolecules* **1997**, *30*, 6764–6770.

(20) Zhang, L.; Eisenberg, A. *J. Am. Chem. Soc.* **1996**, *118*, 3168–3181.

(21) Zipfel, J.; Lindner, P.; Tsianou, M.; Alexandridis, P.; Richtering, W. *Langmuir* **1999**, *15*, 2599–2602.

(22) Burke, S.; Shen, H.; Eisenberg, A. *Macromol. Symp.* **2001**, *175*, 273–283.

(23) Harris, J. K.; Rose, G. D.; Bruening, M. L. *Langmuir* **2002**, *18*, 5337–5342.

(24) Petrov, P. D.; Drechsler, M.; Müller, A. H. E. *J. Phys. Chem. B* **2009**, *113*, 4218–4225.